

SCEC Technical Report

Proposal 21167

Seismic Moment and Corner Frequency of Ridgecrest Earthquakes Determined with Two Novel Methods

Principal Investigator: William L. Ellsworth
Department of Geophysics, Stanford University

Introduction. It is remarkable that while quantification of earthquake source parameters using physics-based theory has been possible for more than 50 years (Aki, 1966; Brune 1970), almost all earthquakes in our catalogs are only quantified by an empirically derived magnitude. Magnitude has served us well, but by itself is an incomplete description of the earthquake. Seismic moment is only routinely reported by the Southern California Seismic Network for earthquakes of $M_W \geq 3.5$. Measures of the rupture dimension or stress drop are only reported in special studies and are absent for the catalogs. In this work, we are participating in the Community Stress Drop Validation Study, developing new methods for rapid, quantitative assessment of earthquake magnitude and duration using the 2019 Ridgecrest earthquake sequence.

The challenges for making precise and accurate measurements of source parameters are well known and have been the subject of extensive research on methods to improve the reliability of the measurements. Here, we are developing and testing a new method for retrieval of source information from time domain amplitude measurements. The method is inspired by the simplicity and durability of local magnitude (M_L), which despite its well-understood limitations continues to be the primary measure of earthquake size for small to moderate earthquakes in many regions today. We derive a measure of seismic moment and source duration from narrow band measurements of the peak displacement amplitude in the time domain. This requires correction for propagation, just as Richter's M_L scale uses a calibrated "attenuation" relationship. The work is being done in coordination with analysis made using spectral methods for calibration, testing and validation.

Methodological Development.

Inspired by the success and simplicity of local magnitude and the work of Rautian and Khalturin on band pass filtered seismograms, we analyze the spectral content of S-waves using time-domain measurements of maximum displacement amplitude, passed through a set of one-octave band-pass filters between 0.25-32 Hz. We currently focus on the maximum amplitude of the S-wave in each octave band.

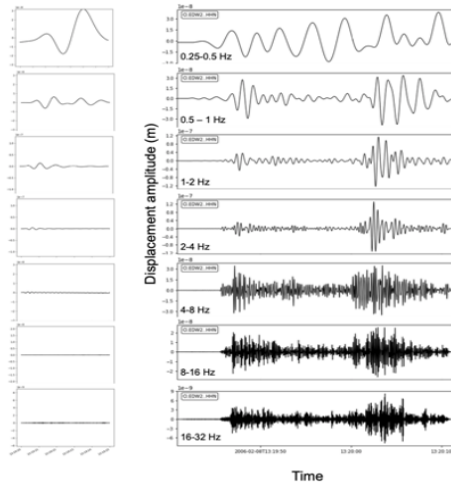


Figure 1. Example of seismogram processing. Each row corresponds to the output of a narrow band Butterworth filter applied to the instrument-corrected displacement seismogram. Left column show pre-event noise at the same scale as the earthquake in the right column. The measurement is simply the peak displacement of the S-wave. Note that signal to noise is easily measured by comparison to the pre-event signal.

To interpret the amplitudes in terms of the source, it is necessary to correct them for propagation effects including geometric spreading, anelastic loss and scattering. We do this by developing an empirical relationship between amplitude and distance in each filter band. The procedure is analogous to the method Richter used to develop the $\log_{10} A_0(\text{epicentral distance})$ attenuation curve for local magnitude (ML). We derived these curves using earthquakes with magnitudes close to MW 3 to minimize the effect of the corner frequency on the results. To correct for the differences in source excitation, we equalized the resulting curves at 10 km distance, as shown in Figure 2 (left). At the lowest frequencies, the curves are close to $1/\text{distance}$, as would be expected for geometric spreading for body waves. We can interpret the curves in terms of Q by assuming the geometric spreading correction. Figure 2 (right) shows the resulting dependence of Q on frequency and distance. Note the strong frequency dependence of attenuation and increase of Q with frequency. Our results are compatible with $Q(f) \sim \sqrt{f}$. For comparison, Raouf, Herrmann and Malagini (BSSA,1999) analyzed $Q(f)$ in southern California and found $Q(f)=180*f^{0.45}$.

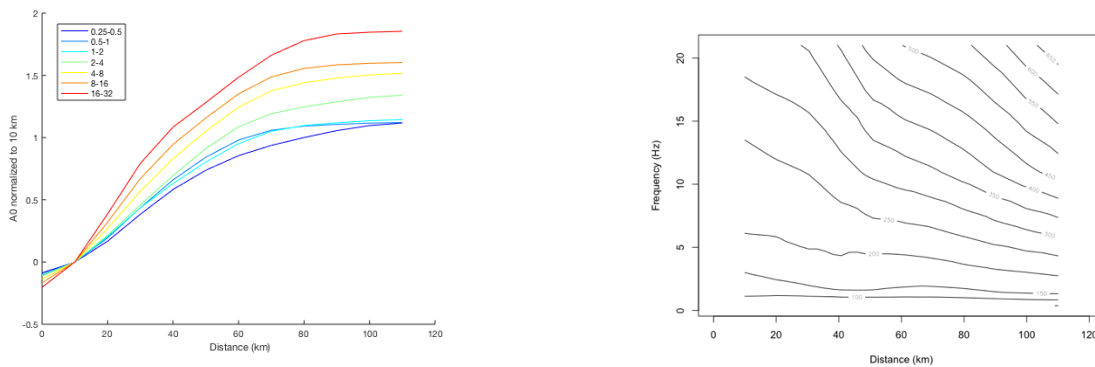


Figure 2. Left: Empirical attenuation curves for the $\log_{10}A(\text{epicentral distance})$ for each frequency band. Curves normalized to 10 km distance. Right: Contour plot of Q as a function of distance and frequency.

Application to Ridgecrest Earthquakes. Maximum amplitudes in each of the 7 octave-wide spectral bands were measured for 309 earthquakes from the Ridgecrest data set with magnitudes between $1.8 \leq ML \leq 4.3$. The observed amplitudes were corrected using the curves shown in Figure 2 (left) as shown in Figure 3. Note that in addition to the collapse of the curves, the apparent corner moves toward a common value and the high frequency asymptotes move toward the expectation of the omega-squared model.

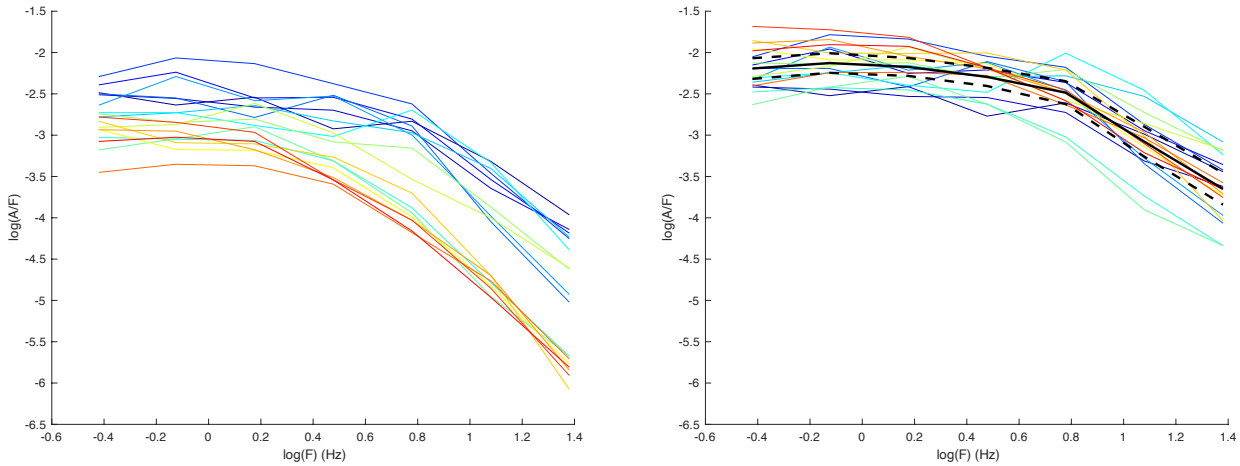


Figure 3. Example of the band-pass amplitudes before (left) and after (right) correction for attenuation using the empirical curves in Figure 2. The black solid line with the corrected spectra shows the mean and the dotted lines the 95% confidence interval of the mean.

We interpret the median “spectrum” for each earthquake using the omega-squared model by finding the best-fitting long period level and corner frequency. The long period level can be related to the seismic moment through an empirical relation using the MW values from the Trugman catalog being used in the Community Stress Drop Validation Study. Examples of fits are shown in Figure 4.

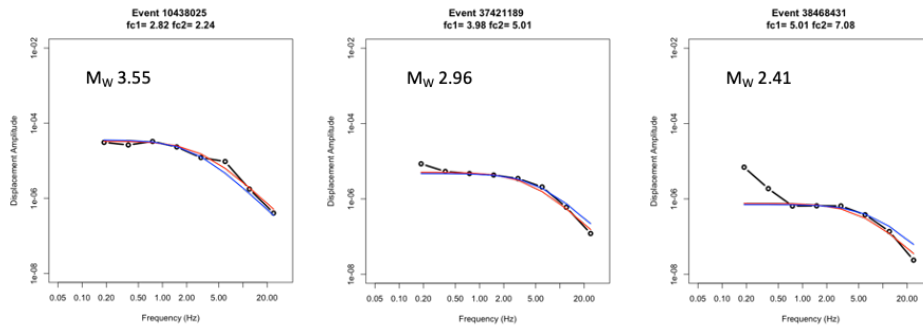


Figure 4. Omega-squared model fit to median amplitude in each frequency band after correction for attenuation. The observations are the black curve, least-square solution using log frequency and log amplitude in red, least-squares solution using linear frequency and amplitudes in blue.

Using the measured long-period levels, after calibration to M_W , we compare our M_0 estimates with those of Trugman () in Figure 5. On average, the two estimates agree well with one another, although there are some significant differences at the upper end that need to be understood.

We also compare our calibrated M_W values with M_L from the Southern California Seismic Network, also in Figure 5. We observe generally good agreement between the two magnitudes for events above M_L 3. Below M_L 3 the scaling changes. This is expected and is due to the corner frequency moving across the instrumental corner of the Wood-Anderson response. So, we're particularly encouraged by this result.

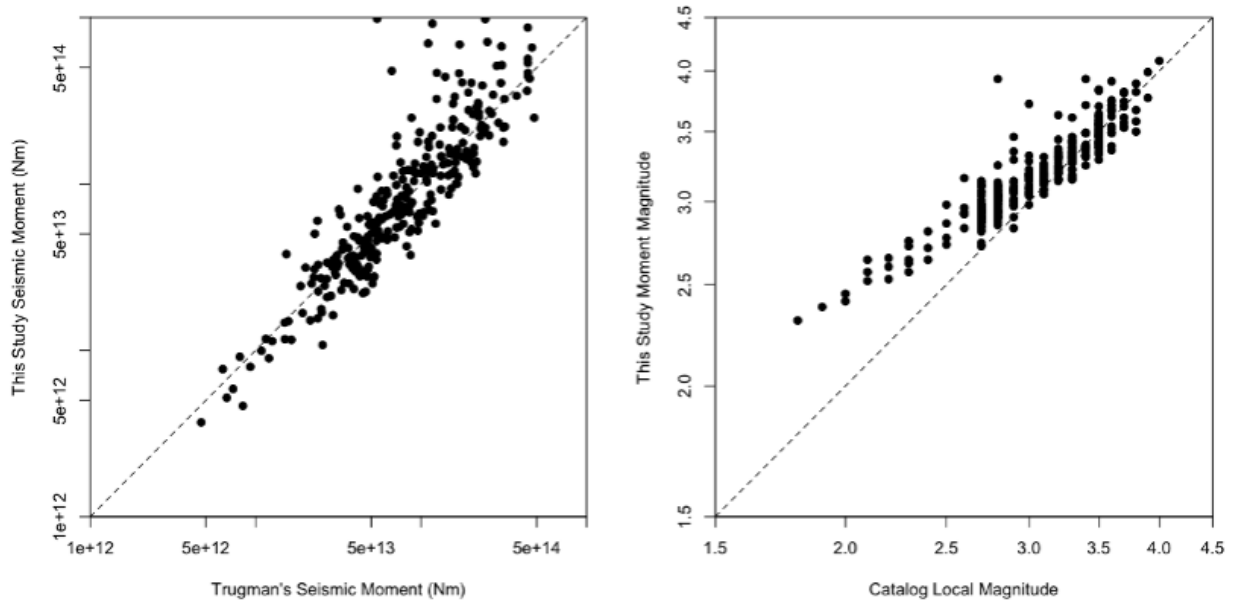


Figure 5. Left: Comparison between Trugman’s seismic moment measurements and those determined in this study. Right: Comparison between catalog M_L and determined in this study from the calibrated seismic moments.

The corner frequencies measured using this approach are approximately 2x too small. We do not fully understand the reason, but think that the octave-wide pass-bands may be too wide. We are in the process of exploring narrower bands and filters with a steeper fall-off than the 3rd order Butterworth filters used thus far.

Next Steps. We are in the process of gathering amplitude data on more events from the test data set, including the 56 event test set identified by the project. We will measure amplitudes using a range of pass bands and filters to determine if the corner frequency can be reliably recovered. We will also derive a model for scaling of M_L to M_W for the Ridgecrest sequence. Once procedures are established, we plan to analyze the complete Ridgecrest sequence for comparison to other methods for measuring source parameters.